Title	Charge transport in a CoPt3 nanocrystal microwire
Authors	Beecher, Paul;De Marzi, Gianluca;Quinn, Aidan J.;Redmond, Gareth;Shevchenko, E. V.;Weller, H.
Publication date	2004
Original Citation	Beecher, P., Marzi, G. D., Quinn, A. J., Redmond, G., Shevchenko, E. V. and Weller, H. (2004) 'Charge transport in a CoPt3 nanocrystal microwire', Applied Physics Letters, 85(23), pp. 5706-5708. doi: 10.1063/1.1830684
Type of publication	Article (peer-reviewed)
Link to publisher's version	http://aip.scitation.org/doi/abs/10.1063/1.1830684 - 10.1063/1.1830684
Rights	© 2004 American Institute of Physics.This article may be downloaded for personal use only. Any other use requires prior permission of the author and AIP Publishing. The following article appeared in Beecher, P., Marzi, G. D., Quinn, A. J., Redmond, G., Shevchenko, E. V. and Weller, H. (2004) 'Charge transport in a CoPt3 nanocrystal microwire', Applied Physics Letters, 85(23), pp. 5706-5708 and may be found at http://aip.scitation.org/doi/abs/10.1063/1.1830684
Download date	2024-04-19 01:19:55
Item downloaded from	https://hdl.handle.net/10468/4397

Charge transport in a $CoPt_3$ nanocrystal microwire

P. Beecher, G. De Marzi, A. J. Quinn, and G. RedmondE. V. Shevchenko and H. Weller

Charge transport in a CoPt₃ nanocrystal microwire

P. Beecher, G. De Marzi, A. J. Quinn, and G. Redmond[a]
Nanotechnology Group, NMRC, Lee Maltings, Prospect Row, Cork, Ireland

E. V. Shevchenko and H. Weller
Institute of Physical Chemistry, University of Hamburg, D-20146 Hamburg, Germany

The electrical characteristics of single CoPt₃ nanocrystal microwires formed by magnetic field-directed growth from colloidal solutions are presented. The wires comprise disordered assemblies of discrete nanocrystals, separated from each other by protective organic ligand shells. Electrical data indicate that the activated charge transport properties of the wires are determined by the nanocrystal charging energy, governed by the size and capacitance of the individual nanocrystals. Focused ion beam-assisted deposition of Pt metal at the wire-electrode junctions is employed to optimize the wire-electrode contacts, whilst maintaining the nanocrystal-dominated transport characteristics of these one-dimensional nanocrystal structures. © *2004 American Institute of Physics.* [DOI: 10.1063/1.1830684]

The unique size-dependent optical and electronic properties of chemically synthesized metal and semiconductor nanocrystals have stimulated intense research interest in recent years.[1–3] These "artificial atoms" have been used to form two- and three-dimensional (2D, 3D) superlattices that exhibit such effects as single electron charging, spin-dependent transport, and insulator to metal transitions.[4–10] They have also been employed as versatile building blocks in the formation of one-dimensional (1D) nanostructures using a variety of methods.[11–15] However, measurement of the charge transport properties of small wires is often hampered by the difficulty involved in achieving good quality wire-electrode contacts. Various techniques have been proposed to minimize the contact resistance problem: Electron beam irradiation or "welding,"[16] fabrication of wire end caps,[17] and metal junction deposition by focused ion beam (FIB).[18] In this letter, we explore the dc electrical characteristics of single CoPt₃ nanocrystal microwires, both as-deposited on contacting electrodes and also following FIB-assisted deposition of Pt metal junctions at the wire-electrode contacts.

6.8-nm-diam CoPt₃ nanocrystals were synthesized via the simultaneous thermal decomposition of cobalt carbonyl and reduction of platinum acetylacetonate by a long-chain 1,2-diol, and stabilized by 1-adamantanecarboxylic acid and hexadecylamine capping ligands using a method described previously.[19] As-synthesized nanocrystals are air-stable to 200 °C, monodisperse (size dispersion $\sigma = 7\%$), uniformly spherical and highly crystalline, possessing a chemically disordered fcc structure. Nanocrystal wires were formed following slow diffusion of a nonsolvent (methanol) into a solution of CoPt₃ nanocrystals in toluene under the influence of an external perpendicular magnetic field (0.9 T) over a period of a week. The wires were typically 10 μm long and 1–2 μm in diameter. High resolution scanning electron microscopy (SEM) analysis of these wires revealed no long-range ordering of nanocrystals at the surface; see Fig. 1(a). The wires are essentially glassy solids where each nanocrystal remains a discrete entity, separated from its neighbors by

a protective coating of organic ligands. A mean internanocrystal separation of $s \approx 1.7 – 1.8$ nm is estimated by counting nanocrystals in a defined area of a SEM image. For measurements of electrical transport through nanocrystal wires, laterally patterned parallel gold electrodes were fabricated on thermally oxidized Si wafer chips using optical lithography followed by metal evaporation (Cr 5 nm/Au 25 nm) and lift
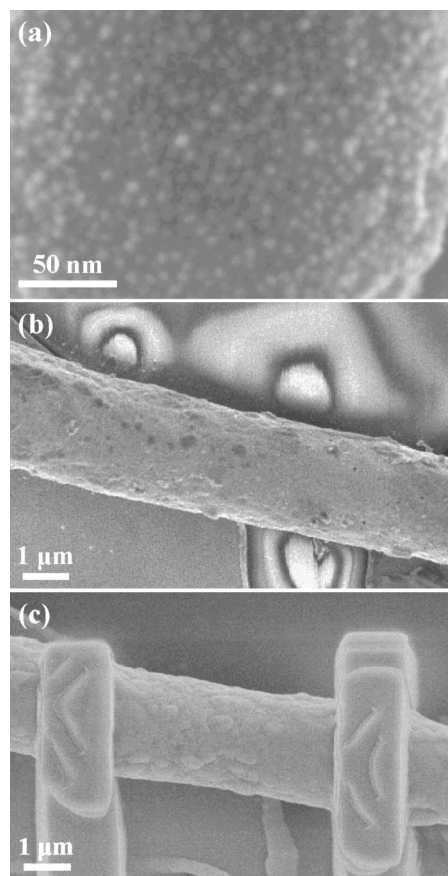

FIG. 1. (a) SEM image of a typical nanocrystal microwire surface. (b) SEM image of an as-deposited nanocrystal wire aligned across a 3-μm-wide electrode gap using a 0.1 T magnetic field. (c) SEM image of the same wire following FIB deposition of metal junction contacts.

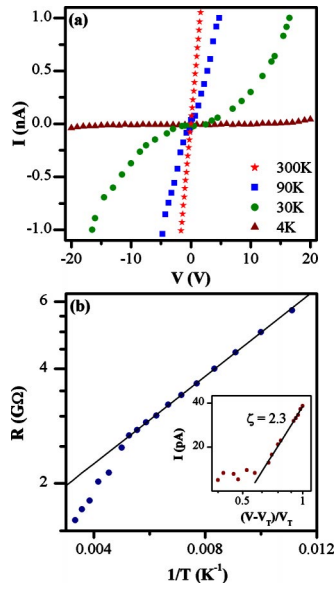[a]Author to whom correspondence should be addressed; electronic mail: gareth.redmond@nmrc.ie

FIG. 2. (Color online) (a) I–V characteristics of the as-deposited microwire device at T=300, 90, 30, and 4 K. (b) Plot of low-bias resistance R vs $1/T$ for this device. Data (circles) are well fit by theory (solid line) for $k_B T < E_c$(11.4 meV). Inset: Above V_T(10 V), the current displays a power-law dependence with a scaling exponent, measured at 4 K, of $\zeta \approx 2.3$.

off, with interelectrode gaps ranging from 1 to 5 μm in width. Devices were prepared by the alignment of wires, in alcohol suspension, perpendicular to the interelectrode gaps using a magnetic field ($\sim$0.1 T), followed by solvent evaporation.

Current–voltage (I–V) characteristics measured for an as-deposited wire device at room temperature exhibited weak nonlinearity with a low bias resistance, $R \sim 1.5$ GΩ (corresponding resistivity, $\rho \sim 3 \times 10^3$ Ω m), which increased monotonically with decreasing temperature. Increased nonlinearity was observed in measured I–V data near zero bias as the temperature (T) was decreased. For $T \leq 30$ K, current suppression was observed at low bias ($R > 500$ GΩ), i.e., a finite threshold voltage, V_T, was required to pass current through the wire.[7,8] For the device with I–V data shown in Fig. 2, a V_T=10 V was observed at 4 K. The temperature dependence of the low bias resistance, R, above 80 K is consistent with the Neugebauer–Webb model for tunnel transport through an array of nanoscale metallic islands with minimal size disorder, where the tunneling rate is temperature-independent but the carrier density is activated.[20] Low-bias electrical transport is therefore dominated by the activation energy, E_c, required to electrostatically charge individual electrically neutral nanocrystals within the wire. Consequently, the measured variation in R with temperature should show activated behavior ($R \propto \exp[E_c/k_B T]$) for $k_B T < E_c$, where k_B is the Boltzmann constant.[7] A semi-log plot of R vs $1/T$ for the as-deposited wire device indicates that the microwire exhibits activated behavior in the temperature range 90–190 K; see Fig. 2(b). The data fit yielded an activation energy, E_c =11.4$\pm$0.1 meV.

The total capacitance of an individual nanocrystal, C_Σ, may be determined via the relation $E_c = e^2/2C_\Sigma$. From the activation energy value obtained above for nanocrystal charging, E_c=7 meV, the total capacitance of each nanocrystal is =7 aF. C_Σ is the sum of the internanocrystal capaci-

tance, C_{nn}, and the nanocrystal self-capacitance, C_0 $\approx 4\pi\varepsilon_0\varepsilon r \approx 1$ aF, where r is the nanocrystal radius (r =3.4 nm), and ε is the relative permittivity of the organic spacers between the nanocrystals, ($\varepsilon \sim 2.7$).[21] For a 2D–3D film with fcc packing, each nanocrystal will have between 6 and 12 nearest neighbors. It is assumed that each nanocrystal has on average 9 nearest neighbors as a result of the disordered packing of nanocrystals in the wire. Neglecting the small contribution to C_Σ from C_0, the mean pairwise inter-nanocrystal capacitance is estimated to be $C = C_{nn}/9$ ≈ 0.8 aF. From this value, the mean internanocrystal spacing, s^*, may then be calculated from the extracted pairwise internanocrystal capacitance using C $\approx 2\pi\varepsilon_0\varepsilon r \ln(1+2r/s^*)$.[7,22] A value of $s^* \approx 1.9$ nm is estimated, in good agreement with the calculated mean internanocrystal separation obtained from SEM data (s =1.7–1.8 nm).

Concerning the voltage dependence of the current below 30 K, for $V > V_T$, theory predicts that for a uniform array of identical nanoscale metallic islands separated by tunnel barriers, the current should follow a power law, $I \propto (V/V_T - 1)^\zeta$, where the scaling exponent, ζ, depends on the dimensionality of the accessible current paths through the wire.[23] For 2D current-carrying networks, theory predicts ζ=5/3, while numerical simulations yield values of $\zeta \approx 2\pm0.2$. Figure 2(b), inset, shows a log–log plot of data measured for the CoPt$_3$ wire yielding a calculated value of ζ=2.3$\pm$0.05. This result suggests that charge transport in the as-deposited wire device is largely 2D, although the microwire-electrode contact resistance may well mask the intrinsic wire characteristics by restricting the number of conducting paths through which charge can flow. To address this issue, disordered platinum metal contacts were deposited onto the regions where the nanocrystal wire crossed over the Au electrodes by direct-write using a FIB system (FEI Vectra 200DE, 10 pA beam current, 10 nm nominal spot diameter, 30 kV acceleration voltage); see Fig. 1(c). Only one FIB image was acquired for alignment purposes prior to contact deposition, so as to minimize exposure of the wire to the highly energetic Ga ion beam.

By this technique, it was possible to decrease the contact resistance and to increase the tunneling current passing through the wire. Figure 3(a) shows the electrical behavior of the FIB-contacted wire measured as a function of temperature. Weak nonlinearity was again observed at room temperature, this time with a vastly reduced low-bias resistance, four orders of magnitude lower than that of the as-deposited wire device, $R \sim 70$ kΩ($\rho \sim 1.3 \times 10^{-1}\Omega$ m). As with the as-deposited device, the low-bias resistance increased monotonically with decreasing temperature. Increased nonlinearity was also observed in the measured I–V data near zero bias as the temperature was decreased. Complete low-bias current suppression occurred at $T \approx 4$ K. The threshold voltage, V_T, required to pass current through the FIB-contacted microwire at 4 K was found to be substantially lower than that measured for the as-deposited wire device; a $V_T \approx 0.5$ V was observed. This reduction in threshold voltage may be associated with a change in the local charge environment of the nanocrystals of which the wire is composed, possibly following exposure to the Ga ion beam employed during imaging of the wire within the FIB system, prior to contact deposition.[8] In this regard, effects on wire resistivity due to
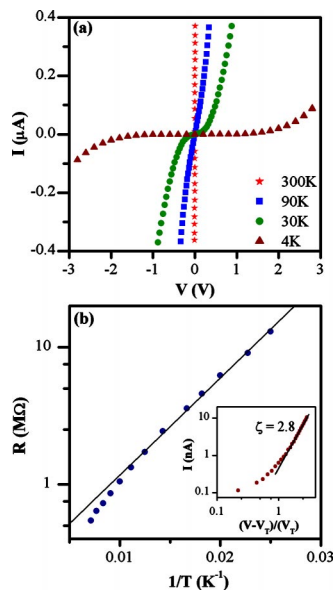
FIG. 3. (Color online) (a) $I–V$ characteristics of the FIB-contacted microwire device at $T=300$, 90, 30, and 4 K. (b) Plot of low-bias resistance R vs $1/T$ for this device. Data (circles) are well fit by theory (solid line) for $k_B T < E_c (\approx 14 \text{ meV})$. Inset: Above $V_T (0.5 \text{ V})$, the current now displays a power-law dependence with a scaling exponent, measured at 4 K, of $\zeta \approx 2.8$.

nanocrystal assemblies where each nanocrystal remains a discrete entity, separated from its neighbors by a protective coating of organic ligands. Electrical characterization data support these observations indicating that the activated charge transport properties of the wires are determined by the nanocrystal charging energy, governed by the size and capacitance of the individual nanocrystals of which the wires are composed. FIB-based deposition of Pt metal at the wire-electrode junctions may be employed to optimize the wire-electrode contacts, improving device fabrication yield while retaining the nanocrystal-dominated transport characteristics of these 1D nanocrystal structures.

Ga ion exposure have previously been observed for bismuth and semiconductor nanowires.[18] The semi-log plot of R vs $1/T$ for the FIB-contacted microwire device exhibited activated behavior in the temperature range 30–130 K, with an activation energy of approximately 14 ± 0.2 meV; see Fig. 3(b). The internanocrystal capacitance extracted using this activation energy value was further estimated to be $C \approx 0.64$ aF. Both values are comparable with those calculated for the as-deposited wire device, thereby confirming that the size-dependent properties of the individual nanocrystals continue to dictate the transport mechanism through the wire after FIB contacting.

The voltage dependence of the current at 4 K, for $V > V_T$, revealed a scaling exponent value of $\zeta = 2.8 \pm 0.05$; see Fig. 3(b), inset. This is a considerably higher value than that obtained for the wire prior to FIB contacting, indicative of transport through networks of conduction paths with dimensionality greater than 2D. A likely reason for this increase in the network dimensionality is that, in this device, the FIB-deposited metal contacts "wrap around" the wire, thereby allowing charge injection into a greater volume of the wire and giving rise to 3D carrier transport within the wire. Therefore, by using the FIB technique for direct-write of metal junctions the quality of the contact between the wire and the electrodes was clearly improved.

In summary, the electrical characteristics of CoPt$_3$ nanocrystal microwires formed by magnetic field-directed growth from colloidal solutions have been presented. Structural characterization indicates that the wires comprise disordered

[1] R. P. Andres, T. Bein, M. Dorogi, S. Feng, J. I. Henderson, C. P. Kubiak, W. J. Mahoney, R. G. Osifchin, and R. Reifenberger, Science **272**, 1323 (1996).
[2] M. M. Alvarez, J. T. Khoury, G. Schaaff, M. N. Shafigullin, I. Vezmar, and R. L. Whetten, J. Phys. Chem. B **101**, 3706 (1997).
[3] S. Chen, R. S. Ingram, M. J. Hostetler, J. J. Pietron, R. W. Murray, G. Schaaff, J. T. Khoury, M. M. Alvarez, and R. L. Whetten, Science **280**, 2098 (1998).
[4] C. B. Murray, C. R. Kagan, and M. G. Bawendi, Annu. Rev. Mater. Sci. **30**, 545 (2000).
[5] C. B. Murray, C. R. Kagan, and M. G. Bawendi, Science **270**, 1335 (1995).
[6] C. P. Collier, R. J. Saykally, J. J. Shiang, S. E. Henrichs, and J. R. Heath, Science **277**, 1978 (1997).
[7] C. T. Black, C. B. Murray, R. L. Sandstrom, and S. Sun, Science **290**, 1131 (2000).
[8] R. Parthasarathy, X. M. Lin, and H. M. Jaeger, Phys. Rev. Lett. **87**, 186807 (2001).
[9] R. C. Doty, H. Yu, C. K. Shih, and B. A. Korgel, J. Phys. Chem. B **105**, 8291 (2001).
[10] K. C. Beverly, J. F. Sampaio, and J. R. Heath, J. Phys. Chem. B **106**, 2131 (2002).
[11] M. T. Reetz, M. Winter, G. Dumpich, J. Lohau, and S. Friedrichowski, J. Am. Chem. Soc. **119**, 4539 (1997).
[12] Z. Tang, N. A. Kotov, and M. Giersig, Science **297**, 237 (2002).
[13] E. Braun, Y. Eichen, U. Sivan, and G. Ben-Yoseph, Nature (London) **391**, 775 (1998).
[14] K. D. Hermanson, S. O. Lumsdon, J. P. Williams, E. W. Kaler, and O. D. Velev, Science **294**, 1082 (2001).
[15] H. L. Niu, Q. W. Chen, H. F. Zhu, Y. S. Lin, and X. Zhang, J. Mater. Chem. **13**, 1803 (2003).
[16] A. Bachtold, M. Henny, C. Terrier, C. Strunk, C. Schonenberger, J. P. Salvetat, J. M. Bonard, and L. Forro, Appl. Phys. Lett. **73**, 274 (1998).
[17] M. Tanase, D. M. Silevitch, A. Hultgren, L. A. Bauer, P. C. Searson, G. J. Meyer, and D. H. Reich, J. Appl. Phys. **91**, 8549 (2002).
[18] S. B. Cronin, Y. M. Lin, O. Rabin, M. R. Black, J. Y. Ying, M. S. Dresselhaus, P. L. Gai, J. P. Minet, and J. P. Issi, Nanotechnology **13**, 653 (2002).
[19] E. V. Shevchenko, D. V. Talapin, A. L. Rogach, A. Kornowski, M. Haase, and H. Weller, J. Am. Chem. Soc. **124**, 11480 (2002).
[20] C. A. Neugebauer and M. B. Webb, J. Appl. Phys. **33**, 74 (1962).
[21] M. A. Rampi, O. J. A. Schueller, and G. M. Whitesides, Appl. Phys. Lett. **72**, 1781 (1998).
[22] B. Laiktman and E. L. Wolf, Phys. Lett. A **139**, 257 (1989).
[23] A. A. Middleton and N. S. Wingreen, Phys. Rev. Lett. **71**, 3198 (1993).